HHS Public Access

Author manuscript

Nat Biomed Eng. Author manuscript; available in PMC 2018 June 11.

Published in final edited form as:

Nat Biomed Eng. 2017 ; 1: 818–825. doi:10.1038/s41551-017-0142-5.

A Growth-Accommodating Implant for Paediatric Applications

Eric N. Feins[a,1], **Yuhan Lee**[b,1], **Eoin D. O'Cearbhaill**[b,c], **Nikolay V. Vasilyev**[a], **Shogo Shimada**[a], **Ingeborg Friehs**[a], **Douglas Perrin**[a], **Peter E. Hammer**[a], **Haruo Yamauchi**[a], **Gerald Marx**[d], **Andrew Gosline**[a], **Veaceslav Arabagi**[a], **Jeffrey M. Karp**[b,*], and **Pedro J. del Nido**[a,*]

[a]Department of Cardiac Surgery, Boston Children's Hospital, Harvard Medical School, 300 Longwood Avenue, Boston, MA, 02115, USA

[b]Engineering in Medicine Division, Department of Medicine, Center for Regenerative Therapeutics, Brigham and Women's Hospital, Harvard Medical School, Harvard Stem Cell Institute, Harvard-MIT Division of Health Sciences and Technology, 60 Fenwood Road, Boston, MA 02115, USA

[d]Department of Cardiology, Boston Children's Hospital, Harvard Medical School, 300 Longwood Avenue, Boston, MA, 02115, USA

Abstract

Medical implants of fixed size cannot accommodate normal tissue growth in children, and often require eventual replacement or in some cases removal, leading to repeated interventions, increased complication rates and worse outcomes. Implants that can correct anatomic deformities and accommodate tissue growth remain an unmet need. Here, we report the design and use of a growth-accommodating device for paediatric applications that consists of a biodegradable core and a tubular braided sleeve, with inversely related sleeve length and diameter. The biodegradable core constrains the diameter of the sleeve, and gradual core degradation following implantation enables sleeve and overall device elongation in order to accommodate tissue growth. By using mathematical modeling and ex vivo experiments using harvested swine hearts, we demonstrate the predictability and tunability of the behavior of the device for disease- and patient-specific needs. We also used the rat tibia and the piglet heart valve as two models of tissue growth to demonstrate that polymer degradation enables device expansion and growth accommodation in vivo.

[*]Co-corresponding authors: Pedro J. del Nido, 300 Longwood Avenue, Bader 2nd Floor, Boston, MA 02115, USA. 617-355-8290. pedro.delnido@cardio.chboston.org; Jeffrey M. Karp, 60 Fenwood Road, Boston, MA 02115, USA. 617-817-9174. bwhkarp@gmail.com.

[c]Current Address: School of Mechanical and Materials Engineering, UCD Centre for Biomedical Engineering, and UCD Conway Institute of Biomolecular and Biomedical Research, University College Dublin, Belfield, Dublin 4, Ireland

[1]Co-first authors

Author contributions

E.N.F and Y.L. designed and performed the experiments, analyzed the data, and wrote the manuscript. E.D.O. contributed to the design of experiments. N.V.V., S.S., and I.F. contributed to the design and performance of experiments, and to the analysis of data. D.P., P.E.H., H.Y., A.G., and V.A. contributed to the design of experiments. G.M. contributed to the analysis of data. P.J.d.N. and J.M.K. contributed to experimental design and manuscript preparation, and supervised the overall project. All authors read and edited the manuscript.

Competing interests

E.N.F., Y.L., E.D.O., N.V.V., D.P., P.E.H., H.Y., V.A., J.M.K., P.J.d.N. have a provisional patent application entitled 'Autonomously Growing Implantable Device' (USSN 62/295,768).

Thousands of surgeries are performed annually on children in the United States, and frequently these procedures involve implantation of a medical device to repair anatomic and morphologic defects (1). Existing surgical implants are extremely effective in many cases (2); however, the inability of fixed-size implants to accommodate growth remains a challenge. In paediatric heart surgery, over 1,000 mitral and tricuspid heart valve procedures are performed in the United States each year (1). In many cases regurgitant heart valves are pathologically dilated and must be tightened down to restore normal size and function. This is true across a range of paediatric heart conditions, including endocardial cushion defects, hypoplastic left heart syndrome, congenital mitral regurgitation, and Ebstein's anomaly (3–6). In adults with dilated heart valves, repair is accomplished by implanting a prosthetic ring on the dilated heart valve annulus (7). Prosthetic annuloplasty rings have significantly improved valve repair durability and outcomes in adults (8,9). In paediatrics, however, prosthetic rings cannot be used since their fixed size would restrict valve growth following implantation (10). Paediatric heart surgeons must therefore use less durable, suture-based annuloplasty techniques (11). Sutures are placed around the dilated valve annulus to cinch it down; however, these sutures break or pull through the tissue over time resulting in pathologic re-dilation of the valve and recurrent valve dysfunction. Although a biodegradable annuloplasty ring that fully degrades over several months was recently developed for use in children, long-term outcomes are still questionable since the biodegradable ring loses mechanical integrity over time and may be subject to mechanical failure (12,13). The lack of a suitable prosthetic ring that can reduce and stabilize the dilated paediatric heart valve but then allow for controlled, physiologic growth is a major reason for the limited success of valve repair in children. Successful tricuspid valve repair is achieved in only 50% of children with single-ventricle anatomy, and failed repair is an independent risk factor for mortality (4,14).

Disorders of long-bone growth, including limb-length discrepancy and angular limb deformities, are among the most commonly treated non-traumatic conditions in paediatric orthopedics (15). They can be managed surgically by compression-based growth plate modulation, whereby fixed-size devices (e.g. staples, plated systems) are implanted across the long-bone growth plate to temporarily slow bone growth and gradually correct angular limb deformities and limb length discrepancies (16). Unfortunately, children require additional surgeries for device removal to avoid premature physeal closure, growth arrest, and overcorrection since these devices are fixed in size (17). Additionally, following implant removal children are at risk for rebound growth, which is unpredictable and can require repeat surgical interventions to re-correct recurrent limb deformities (18). Similar strategies of growth plate modulation are used to treat scoliosis – another of the most common paediatric orthopedic conditions requiring surgery, with several thousand surgeries performed each year. An estimated 17,000 surgeries are performed annually to treat scoliosis in the United States (1,19). Staples and vertebral body tethering systems are implanted along the convex side of the spine to asymmetrically restrict growth and allow the concave side to "catch up" (20). However, with these fixed-size implants overcorrection of the spine can occur requiring repeat surgical interventions for device revision/lengthening (21,22). An implantable device with autonomous elongation potential could obviate the need for some

re-interventions in children by accommodating physiologic growth after skeletal deformity correction.

Here we demonstrate a growth-accommodating device that employs a tubular braided sleeve and a biodegradable core. Sleeve length and diameter are inversely related due to the intrinsic geometry of the braid, so that thinning out of the sleeve results in elongation. This phenomenon has been exploited for pneumatic muscle actuators in soft robotics, where pneumatic expansion/contraction of an elastic bladder effects shortening/lengthening of a surrounding braided mesh to mimic muscle contraction/elongation (23). In the current concept, sleeve diameter is instead controlled by an inner biodegradable core, so that polymer core degradation is coupled to braid length and overall device elongation (Fig. 1a). The device is designed to initially constrict pathologically dilated tissue and correct the contours of malformed structures, as is needed during heart valve repair and correction of skeletal deformities. As the core degrades following implantation the braided sleeve can thin out and elongate in response to surrounding tissue growth without requiring additional interventions. Importantly, the device design comprises only two principle elements, which helps promote device durability.

We demonstrate tunability and predictability of device behavior based upon the structural and chemical parameters of the braided sleeve and biodegradable core. By altering braid geometry and polymer degradation rate, we could modify the device elongation profile to target a range of paediatric applications. To maintain the device's mechanical strength throughout polymer core degradation and ensure conformability around different tissue/organ contours, we used the surface-eroding, biodegradable, biocompatible polymer poly(glycerol sebacate) (PGS), which can possess the requisite mechanical properties to resist compressive forces from the braided sleeve (24). The mechanical strength of the device was sufficient to withstand physiologic stresses in two distinct *in vivo* environments. Using two animal models we demonstrate that the device concept can initially constrict tissue following implantation but then accommodate native growth without requiring additional interventions.

Autonomous growth-accommodation – coupling core degradation to braid elongation

The ideal growth-accommodating device should: (*i*) achieve tissue/organ repair like current fixed-size devices, (*ii*) gradually and continuously elongate in concert with native tissue growth in children, (*iii*) possess a tunable and predictable elongation profile to enable disease- and patient-specific application, (*iv*) be mechanically strong enough to withstand physiologic stresses throughout growth after implantation, (*v*) possess a non-degradable element that remains implanted to provide long-term tissue support once the organ has completed growth, and (*vi*) be simple in design to facilitate rapid translation to clinical application. We chose a biaxial braid as the outer sleeve construct because the transformation of diameter change into length change can be precisely tailored to generate distinct elongation profiles, enabling better design flexibility. Braided sleeves enable the coupling of inner core degradation to overall device elongation: they are porous enough to

allow access of body fluids to the biodegradable polymer core for hydrolytic degradation, but strong enough to stably contain the core.

To demonstrate how degradation of a surface-eroding core could be coupled to braid elongation to achieve gradual autonomous device elongation, we performed expedited *ex vivo* experiments in a water tank setup. 1-dimensional (1-D) and 2-dimensional (2-D) device expansion were studied since they resemble long bone and heart valve growth, respectively. For the 1-D experiments a biaxial nitinol braided sleeve (Creganna Medical) was tied down on either side of a spherical sucrose core. The sucrose core was used as an expedited alternative to surface-eroding polymers with significantly slower degradation rates. The braid/core device was exposed to a 2 N tensile force to mimic the external forces of tissue growth, and then submerged in room temperature water. Core diameter gradually decreased over 55 minutes as the sugar core dissolved underwater which enabled gradual elongation of the braided sleeve in response to the tensile force (Fig. 1b,c). This mimicked an orthopedic device implanted along a growing long bone that could initially limit and guide bone growth following implantation, but then could elongate to accommodate normal growth.

As a 2-D growth model, a device prototype was implanted around the tricuspid valve annulus in an *ex vivo* isolated swine heart preparation, in which physiologic cardiac pressures were generated (Supplementary Fig. 1). A rudimentary annuloplasty ring, comprised of an ethylene chlorotrifluorethyelene (ECTFE) co-polymer biaxially braided sleeve and heat-molded spherical sugar cores, immediately reduced the tricuspid valve annular area by approximately 25%, analogous to existing annuloplasty ring repairs (Fig. 1d). Placing the heart and device in room temperature water enabled dissolution of the inner spherical cores. Degradation of the core allowed braided sleeve elongation, and re-expansion of the tricuspid valve annulus in a gradual and predictable manner akin to native heart valve growth in children (Fig. 1e) [Movie S1]. In both *ex vivo* experiments core degradation was coupled to braided sleeve diameter and overall device length, thus creating a mechanism of autonomous device elongation and obviating the need for additional interventions to enlarge, elongate, or replace the device. Importantly, device elongation, and thus surrounding tissue growth, could be controlled solely by degradation of the core.

Analytical model for fine-tuning braid behavior

To fine-tune the growth-accommodating device for paediatric use, a mathematical model describing braided sleeve behavior was employed (25). Braid parameters affecting the elongation profile include: initial sleeve length (L_i), initial sleeve diameter (D_i), instantaneous sleeve diameter (D), and pitch (i.e. number of fiber turns, n, per unit length). With these inputs sleeve length (L) was defined as a function of sleeve diameter (equation (1)):

$$L(D) = \sqrt{\left((\pi n D_i)^2 + L_i^{\,2} - (\pi n D)^2\right)} \quad (1)$$

Adjusting braid pitch (n) created of a range of unique elongation profiles, with higher pitch enabling greater length change for a given change in degradable core diameter. Based on the

model, devices assembled using a 2 mm core with braid pitches of 46, 54, and 60 ppi (picks-per-inch) could elongate by 38.4%, 50.6%, and 62.8%, respectively. Experimentally measured sleeve lengths correlated well with predicted elongation curves ($R^2 > 0.99$) (Fig. 2a). This demonstrated how the use of a braid as the outer element imparts tunability and predictability on the device concept.

Polymer development & device characterization

The degradable core should have controlled size/shape change throughout degradation and maintain a high compressive modulus in order to resist compressive deformation by the outer braided sleeve under tension, thus allowing device elongation only in response to polymer degradation. We selected the tough elastomer PGS – a hydrophobic surface-eroding polymer that exhibits minimal swelling in water and maintains its structural integrity throughout degradation, in contrast to bulk-eroding polymers and hydrophilic polymers whose mechanical strength deteriorates during degradation (26). Although PGS met most of the design criteria, existing PGS was too soft to resist compressive deformation by the outer braided sleeve under tension from different tissues (e.g. bone, heart valve annulus) (27). For example, rat tibial growth generates approximately 0.83 MPa of tensile stress (28). Conventional PGS, with a tensile modulus of ~0.5 MPa, would allow the device to stretch by more than 50% without ever degrading and would therefore not be suitable for controlling braid dimensions and restricting abnormal bone growth. To minimize stretching to less than 5%, extra-stiff PGS (ESPGS) was synthesized using unique reaction conditions to maximize polymer crosslinking (155°C for 86 hours in vacuum) within cylindrical polytetrafluoroethylene (PTFE) molds (29). In accelerated degradation studies using strong base (0.1 M NaOH solution in water, pH 13.0), the reaction temperature dramatically changed the degradation profile (Fig. 2b). The degradation rate of ESPGS was 9.2-fold slower than that of conventional PGS, suggesting that complete degradation of ESPGS in physiological conditions could be adjusted depending upon the clinical application.

To assess the mechanical strength of a fully assembled device, ESPGS was inserted into an ultra-high-molecular-weight polyethylene (UHMWPE) braided sleeve and tested using a universal mechanical tester. ESPGS dramatically increased device modulus. Fig. 2c demonstrates the relationship between polymer curing time (at 155°C) and device modulus. Lengthening the curing time significantly enhanced device stiffness. When ESPGS was cured for 86 hours, the overall device modulus reached 173 MPa, exceeding the compressive modulus of conventional PGS and surpassing the Young's modulus of commercially available surgical sutures (e.g. PTFE and polydioxanone) (30). To evaluate device fatigue, cyclic fatigue testing was performed. This showed that there was no fatigue related to the braided sleeve or the ESPGS core, which was critical for ensuring that controlled polymer core degradation, rather than polymer deformation, was responsible for device elongation (Fig. 2d).

Ex vivo testing was also performed to determine the effect of compressive stress on polymer core degradation. Device prototypes comprising a 1.8 mm ESPGS core and an outer UHMWPE braid sleeve were placed in a 0.1 M NaOH solution and exposed to varying magnitudes of tensile stress (applied to the ends of the braid). Given the nature of the braid,

a tensile stress applied to the braid translated to a compressive stress on the polymer core. Importantly, the amounts of stress applied to the devices were similar to those experienced at the growth plate (28). The rate of polymer erosion was determined by measuring the polymer core diameter at various time points after initiating the experiment. Tensile stress on the braid had no impact on core degradation rate, which is an important feature since it means core degradation is predictable regardless of how much stress is applied (Fig. 2e).

In vivo bone growth model

To demonstrate proof-of-principle of autonomous device elongation and tissue growth accommodation in an *in vivo* environment, a rat tibial bone growth model was developed. Young, growing male Wistar rats (150-200g) underwent surgical implantation of a device prototype along the left tibia, analogous to conventional implants used to guide bone growth in children, and were survived for eight weeks (Supplementary Fig. 3). Three animals received a growth-accommodating device with a degradable ESPGS core, and three animals received a fixed-size device with a non-degradable PTFE core, akin to existing implants (Fig. 3a). The right tibia served as a control. All animals underwent interval micro computed-tomography (CT) imaging to evaluate tibial growth.

Micro-CT images of the tibia and device in axial and sagittal cross-sections demonstrated the contrasting behavior of the elongating and fixed-size devices over 8 weeks. In animals receiving a device with a nondegradable core, overall device length remained fixed (Fig. 3b), which was confirmed on direct examination at the time of explant (Fig. 3c). In animals receiving a device with a degradable ESPGS core, the core became progressively thinner with degradation, and overall device length increased (Fig. 3d). Examination at explant confirmed this device elongation (Fig. 3e).

Importantly, device behavior translated to distinct tibial growth profiles for the two animal groups when compared to the contralateral (right) limb (Fig. 3f). PTFE animals experienced significant and progressive growth restriction. Overall growth was only 20.0% over 8 weeks compared with 32.0% growth in the unrestricted, right tibia ($p = 0.006$). There was near arrest of left tibial growth in the final 4 weeks of survival: 2.6% left tibial growth versus 7.1% growth in the right tibia ($p = 0.01$). By the end of the study left tibial length in PTFE animals was significantly shorter than right tibial length ($p = 0.004$). The distinct growth trends in the final 4 weeks suggest that further growth differential would have occurred had the animals been survived longer. The latter 4 weeks of the study, in principle, represent a time when device removal/exchange would be necessary in a growing child to avoid excessive growth restriction. ESPGS animals, in contrast, experienced continued, guided bone growth, following a more physiologic growth pattern that was nearly identical to right tibial growth in the final 4 weeks (7.3% vs. 7.1%, $p = 0.98$) (Fig. 3f). Arrest of bone growth was avoided because of autonomous device elongation, suggesting that this would prevent the need for device removal/exchange in a growing child.

Based on the device diameter change as measured by micro-CT, the device elongation profile was predicted using the braid elongation model (equation (1)) and compared with the actual device elongation profile (Fig. 3g). Observed device elongation closely correlated

with predicted elongation (19% observed elongation over 8 weeks versus 22.5% predicted elongation). This demonstrated that predictability could be achieved with the braided device concept in an *in vivo* environment.

Proof-of-principle heart valve growth model

We further explored the use of the device on tissues in a more dynamic environment, namely, the heart valve in a growing piglet model. In this preliminary study, four growing, female Yorkshire piglets (mean age 7.3 ± 0.9 weeks) underwent surgical implantation of a growth-accommodating annuloplasty ring prototype on the tricuspid valve and were survived for 5, 12, 16, and 20 weeks to assess device behavior and valve growth. We performed tricuspid valve annuloplasty rather than mitral valve annuloplasty because tricuspid valve surgery can be performed with the heart still beating and with lower risk of systemic embolism. It was therefore felt that tricuspid surgery would be better tolerated by the piglets. We fabricated the growth-accommodating annuloplasty device to have a similar geometry to commercially available, fixed-size annuloplasty rings (Fig. 4a). The novel ring prototype was meant to reduce valve size at implantation akin to existing rings, and then expand to accommodate valve growth.

Valve size was measured with epicardial 3-dimensional (3-D) echocardiography immediately before and after ring implantation, and at the time of euthanasia. Fig. 4b shows the growth-accommodating ring prototype comprised of an UHMWPE braided sleeve over a curved cylindrical ESPGS core. Fig. 4c shows a magnified view of the sleeve's biaxial braid configuration. The ring was implanted using the standard technique for ring implantation in adults: the ends of the braided sleeve were anchored to the valve annulus with sutures, and additional sutures were placed through the valve annulus and around the ring along its length (Fig. 4d). This enabled downsizing of the annulus and apposition of the ring to the annulus, as is typically achieved in heart surgery. At the time of euthanasia, hearts were explanted to assess device fixation and ESPGS degradation.

In all cases the ring remained well affixed to the valve annulus throughout the survival periods without evidence of dehiscence (Fig. 4e). This was likely promoted by the development of a collagen tissue layer over the device following implantation (Fig. 4f). ESPGS degradation was observed on direct inspection of explanted core segments (Fig. 4g). Cross-sections through explanted ring segments demonstrated areas of significant polymer core erosion following implantation (Fig. 4h, top), although there was regional variation with some segments experiencing less extensive core erosion (Fig. 4h, bottom). Echocardiographic evaluation showed that the tricuspid valve in each animal was effectively downsized by the growth-accommodating ring prototype at the time of surgery (Fig. 4i, *pre-implant* to *post-implant*). This demonstrated that the ring could withstand intra-cardiac forces and effectively constrain the valve, as is necessary in heart valve repair surgeries. Valve reduction was then followed by valve growth after device implantation (Fig 4i, *post-implant* to *euthanasia*), although the growth rate varied among the animals. Valve function was assessed with 2-D color Doppler and continuous wave Doppler epicardial echocardiography before and after ring implantation, and at the time of euthanasia, looking specifically for evidence of tricuspid valve stenosis, regurgitation, and peri-prosthetic leak.

In all animals, valve function remained well-preserved with low velocity, laminar blood flow across the valve and no significant transvalvular gradient to suggest the development of tricuspid valve stenosis (Fig 4j). Additionally, there was no evidence of significant leaflet regurgitation or peri-prosthetic leak around the rings. This initial proof-of-concept study demonstrated the potential for controlling heart valve growth with core degradation using the growth-accommodating device concept.

Discussion

Many existing fixed-sized surgical implants suffer limitations for paediatric use due to their inability to accommodate growth. In paediatric orthopedics, fixed-size implants often require repeated interventions for removal or replacement to avoid excessive growth restriction. In paediatric heart valve surgery, fixed-size annuloplasty rings are avoided altogether given the risk of causing valve stenosis.

We demonstrate a concept for autonomous device elongation utilizing a biodegradable core that gradually decreases its diameter via surface erosion and an outer biaxially braided sleeve that transforms core diameter reduction into gradual, longitudinal device expansion to accommodate native tissue growth. *Ex vivo* and *in vivo* experimentation validated the concept of coupling polymer degradation to braided sleeve behavior to achieve autonomous device elongation. In the presence of polymer core degradation, normal tissue growth was observed, while the absence of core degradation was associated with significant growth restriction. This demonstrated the link between device core degradation and growth accommodation.

The development of ESPGS was important for creating a device strong enough to withstand *in vivo* forces in humans. The human tibia generates approximately 1 MPa of compressive stress at the growth plate (31). As in the rat, this amount of stress would cause minimal device strain (~3%), suggesting that the ESPGS device would be sufficiently strong for orthopedic applications. The *in vivo* tensile stress on a prosthetic annuloplasty ring reaches approximately 5 MPa (32). This higher magnitude stress is caused by the dynamic, beating heart; it can be inferred that slow and gradual cardiac tissue growth would generate much smaller stresses on a prosthetic ring that would not be sufficient to cause significant device strain. The braid/ESPGS ring would therefore only elongate in response to polymer degradation and would enable predictable, guided tissue growth. Importantly, in vitro studies also showed preservation of device strength after partial degradation, so even as the polymer core degraded the device would remain strong enough to withstand in vivo forces (Supplementary Fig. S2c).

Testing the device in two distinct *in vivo* models demonstrated how the surrounding microenvironment impacts device behavior. In the orthopedic rat model device elongation correlated with ongoing bone growth throughout the study period. Notably, even with a fixed-size implant there was some bone growth in the first 4 weeks of survival. This is explained by two factors: (*i*) despite aiming to implant the device under tension there was inevitably some slack in the implant that allowed for some degree of initial unrestricted

growth, and (*ii*) the tibia has two growth plates (proximal and distal) and the device only crossed the proximal growth plate, thus allowing for some growth at the distal growth plate.

In the swine heart model polymer erosion and ring diameter decrease were observed, albeit to variable degrees (Fig. 4h). Some segments experienced more dramatic erosion and diameter decrease than others. This is in contrast to the rat bone growth model, where polymer erosion and device elongation were fairly uniform along the device (Fig. 3d,e). The ideal device should undergo uniform core degradation and device elongation, and this will be a focus of future work. However, it is important to recognize that valve growth was accommodated in all animals despite core degradation not being perfectly uniform. Moreover, valve function was preserved without the development of valve stenosis, leaflet regurgitation, or peri-prosthetic leak. This variability in polymer erosion may be partly explained by the growth of a collagen layer on the ring, which may have reduced access of water molecules and/or enzymes to the device, therefore slowing ESPGS degradation. Any variability in collagen overgrowth could have caused regional differences in core degradation and device expansion. Notably, in previous studies of subcutaneous PGS implantation formation of a thin fibrotic capsule was observed, but PGS still fully degraded over weeks to months (27,33). This suggests that our growth-accommodating device concept, despite inducing collagen overgrowth, would continue to experience core degradation, albeit at a slower rate.

There are several ways to modify the sleeve and polymer to encourage ongoing core degradation and device elongation. The number and thickness of braid fibers could be reduced to create a looser braid that would allow greater access of water molecules to the polymer core and facilitate continued polymer degradation. Required overall device strength would have to be considered when making any modifications to braid fiber number or thickness since reducing the number and/or thickness of braid fibers would also reduce the tensile strength of the overall device. Fiber materials with a higher tensile modulus could be considered for this to maintain the device's tensile strength. Use of a different braid material that induced a less pronounced fibrous tissue response could also facilitate ongoing polymer degradation and long-term device elongation. The wide range of available braid materials with unique tissue responses could permit the design of devices with distinct elongation behaviors. ESPGS can also be engineered to adjust degradation profile without compromising the device's overall mechanical strength. Alternative core geometries (e.g., row of spheres) would increase the polymer's surface area-to-volume ratio and could enhance degradation. Future work is required to further characterize *in vivo* device behavior, focusing on how polymer core degradation is impacted by changes in core geometry and sleeve porosity. This will be important when adjusting the device to target specific clinical applications.

This device concept is somewhat predicated on the ability to predict and approximate the growth rate of a child. In paediatric heart surgery, a Z-scoring system is widely used to normalize heart structures to body surface area. This system is used to appropriately size cardiac implants and help predict future growth (34). In paediatric orthopedics, spinal growth rate is well characterized throughout childhood (35). These growth patterns can be targeted when designing an autonomously elongating device. However, if the predicted

growth rate is not accurate for a given patient, then mismatches might occur between an implanted device and the patient. While small mismatches might be well tolerated, larger mismatches could prove problematic for a child. Additionally since the growth rate of many bodily structures, such as the spine, varies throughout childhood, a device with a single fixed growth rate would be unable to perfectly mirror somatic growth. A potential modification to the device concept involves a core made of several distinct layers, each composed of a unique polymer that possessed a distinct degradation profile. With this type of core, device elongation could be pre-programmed to have different elongation rates at different points following implantation. Even with this modification, the ability to adjust the device following implantation could help alleviate potential patient-implant mismatches. An additional device modification could include light-triggered cleavable bonds in the ESPGS core, so that accelerated degradation could be triggered with external light. Near-infrared light, which can penetrate soft tissues, could be used so that device elongation could be adjusted without repeated surgical interventions. These proposed modifications to the device concept will be the subject of future work.

Importantly, the device concept comprises only two principle elements (a braided sleeve and a biodegradable core) that work closely in concert to enable growth. Having only two principle components should promote device durability since there are no interlocking or moving parts that are prone to breakdown/failure. Notably, *ex vivo* studies demonstrated no evidence of device fatigue, and all *in vivo* devices remained intact throughout the 8-week rat survival period and the 20-week piglet survival period, during which devices were exposed to dynamic biological environments. The flexible nature of the braided sleeve and polymer further contributes to device durability, enabling the device to work in one or more dimensions.

While the braided sleeve and polymer core work in concert to enable growth, they can be independently modified to achieve a range of device elongation profiles that apply to a broad spectrum of clinical applications. In addition to the paediatric cardiac and orthopedic surgeries already described, potential applications exist for esophageal and intestinal atresias. The braid could be engineered to have shape memory, such that as the polymer degraded after implantation in the esophagus or intestine the braid would actively elongate to gradually increase esophageal/intestinal length. Another potential application is for the surgical treatment of mandibular condylar hyperplasia (CH) – a cause of asymmetric facial deformities in the case of unilateral CH and prognathism (an underbite) in the case of bilateral mandibular CH. When implanted on the affected condyle this device could limit growth due to CH but then elongate to allow for normal mandibular growth. This could potentially improve upon existing surgical techniques, which involve either surgical resection to permanently arrest growth or allowing the disease to burn out and then performing delayed surgical correction. (36) The *ex vivo* device characterization and *in vivo* models presented here demonstrate initial proof-of-principle and form the basis for future work to optimize device design for different clinical needs in paediatrics. In this regard, the present work represents the foundation for a new paradigm of paediatric device development.

Materials & Methods

To make ESPGS, a viscous PGS pre-polymer was synthesized via catalyst-free, solvent-free polycondensation of 0.1 mol each of glycerol and sebacic acid at 120°C for 8 hours in a nitrogen environment and for 16 hours in vacuum. The resultant viscous PGS pre-polymer was then injected into thin-walled PTFE tubing (inner diameter = 1.8 mm), which acted as a sacrificial mold, and was then cured in a vacuum oven at 155°C. Samples were cured up to 86 hours to produce 1.8 mm ESPGS cylinders.

For the rat musculoskeletal study, which required a straight device to lie along the tibia, the polymer was cured within the PTFE tubing for all 86 hours. To create curved ESPGS samples for the annuloplasty ring of the swine study, straight polymer cylinders were removed from the PTFE tubing after 42 hours of curing, placed into an appropriate radius of curvature, and cured at 155°C for an additional 44 hours. This division in curing intervals (42 and 44 hours) was chosen because sufficient curing within the straight PTFE tubing was required to produce freestanding polymer cylinders prior to inducing curvature.

Device manufacturing for the rat study involved insertion of the 1.8 mm diameter cylindrical ESPGS or PTFE core into the biaxially braided UHMWPE sleeve. UHMWPE braid was manufactured by Biomedical Structures and had a pitch of 60 ppi, with a 1/1 intersecting pattern (Fig. 4c). Twenty-four fibers were used to construct the braided sleeve, with each fiber being composed of twenty-five 12 nm filaments. Two animals received a PTFE (Gore-Tex®) braided sleeve for micro-CT imaging. Twelve CV-5 Gore-Tex® sutures (W.L. Gore & Associates, Inc.), each 0.246 mm in diameter were braided in a 1/1 intersecting pattern around a 2.1 mm mandrel. After inserting the core inside the braided sleeve, a polypropylene (Prolene®) suture (Ethicon) was tied to each end of the device; these sutures were used to anchor the device to the bone during surgical implantation.

Production of annuloplasty rings for the swine study involved insertion of a curved ESPGS core into a long segment of UHMWPE braided sleeve (Fig. 4b). The braid/ESPGS composite was then attached to a mounting device for surgical implantation, utilizing polyglactin 910 (Vicryl®) sutures (Ethicon) (Supplementary Fig. S4). The mounting device was engineered using SolidWorks design software (SolidWorks) and manufactured with a photoacrylic using an Alaris 30 3-D printer (Objet). All device implants used for *in vivo* experimentation underwent a standard ethylene oxide sterilization process prior to surgical implantation.

Both experimental animal protocols were approved by the Boston Children's Hospital Institutional Animal Care and Use Committee (IACUC). All animals received humane care in accordance with the 1996 "Guide for the care and use of laboratory animals" recommended by the US National Institutes of Health. The experiments did not use a method of randomization. The investigators were not blinded to allocation during experiments and outcome assessment.

Statistical analysis

To determine the correlation between modeled and experimentally measured braided sleeve lengths (Fig. 2a) the Pearson correlation coefficient was calculated. For multiple comparisons, one-way analysis of variance (ANOVA) was performed. If ANOVA yielded a statistically significant result ($P < 0.05$) then a post-hoc Tukey's honest significant difference (HSD) test was performed at significance levels of 95%. Error bars in all graphs represent standard deviation. The power calculation (rat tibia growth experiments) distinguished as significant a difference of 60% in the outcome variable between test and control group; 60% estimated standard deviation; $p = 0.05$; 90% confidence; $n = 3$. No statistical methods were used to pre-determine thesample size of the piglet heart valve experiments. All statistical analyses were performed with StatPlus® software (AnalystSoft Inc.).

Data availability

The authors declare that all data supporting the findings of this study are available within the paper and its Supplementary Information.

Supplementary Material

Refer to Web version on PubMed Central for supplementary material.

Acknowledgments

The authors are grateful to the Animal Research Children's Hospital staff (Arthur Nedder, DVM, and veterinary technicians) and the Boston Children's Hospital perfusion team for their overwhelming support and assistance in this project. This work was also supported by the NIH grant GM086433 to J.M.K., and the Basic Science Research Program through the National Research Foundation of Korea (NRF) funded by the Ministry of Education of Korea (2012R1A6A3A03041166) and Korea Institute for Advancement of Technology (N0002123) to Y.L.

References

1. HCUP Kids' Inpatient Database (KID). Healthcare Cost and Utilization Project (HCUP). Agency for Healthcare Research and Quality; Rockville, MD: 2012. https://hcupnet.ahrq.gov (3/22/15)
2. Lam S, Kuether J, Fong A, Reid R. Cranioplasty for large-sized calvarial defects in the pediatric population: A review. Craniomaxillofac Trauma Reconstr. 2015; 8:159–170. [PubMed: 26000090]
3. Kaza E, et al. Changes in left atrioventricular valve geometry after surgical repair of complete atrioventricular canal. J Thorac Cardiovasc Surg. 2012; 143:1117–1124. [PubMed: 22078711]
4. Honjo O, Mertens L, Van Arsdell GS. Atrioventricular valve repair in patients with single-ventricle physiology: mechanisms, techniques of repair, and clinical outcomes. Semin Thorac Cardiovasc Surg Pediatr Card Surg Annu. 2011; 14:75–84. [PubMed: 21444052]
5. Chavaud S, et al. Reconstructive surgery in congenital mitral valve insufficiency (Carpentier's techniques): Long-term results. J Thorac Cardiovasc Surg. 1998; 115:84–93. [PubMed: 9451050]
6. Dearani JA, et al. Anatomic repair of Ebstein's malformation: lessons learned with Cone reconstruction. Ann Thorac Surg. 2013; 95:220–228. [PubMed: 23200240]
7. Doty, DB., Doty, JR. Cardiac Surgery: Operative Technique. Elsevier; 2012.
8. Parolari A, Barili F, Pilozzi A, Pacini D. Ring or suture annuloplasty for tricuspid regurgitation? A meta-analysis review. Ann Thorac Surg. 2014; 98:2255–2263. [PubMed: 25443026]
9. Tang GH, et al. Tricuspid valve repair with an annuloplasty ring results in improved long-term outcomes. Circulation. 2006; 114(suppl):1577–1581.

10. Choi JB, Kim KH, Kim MH, Kim WH. Mitral valve re-repair in an adolescent patient with prosthetic ring endocarditis: posterior leaflet augmentation and posterior strip annuloplasty. J Card Surg. 2012; 27:560–562. [PubMed: 22978833]
11. Jonas, RA. Comprehensive Surgical Management of Congenital Heart Disease. CRC Press; 2013.
12. Kalangos A, et al. Annuloplasty for valve repair with a new biodegradable ring: An experimental study. J Heart Valve Dis. 2006; 15(6):783–790. [PubMed: 17152786]
13. Bautista-Hernandez V, et al. Atrioventricular valve annular remodeling with a bioabsorbable ring in young children. JACC. 2012; 60(21):2255–2260. [PubMed: 23103041]
14. Lee TM, et al. Risk factor analysis for second-stage palliation of single ventricle anatomy. Ann Thorac Surg. 2012; 93:614–619. [PubMed: 22197533]
15. Friend L, Widmann RF. Advances in management of limb length discrepancy and lower limb deformity. Curr Opin Pediatr. 2008; 20:46–51. [PubMed: 18197038]
16. Goldman V, Green DW. Advances in growth plate modulation for lower extremity malalignment (knock knees and bow legs). Curr Opin Pediatr. 2010; 22:47–53. [PubMed: 19926991]
17. Boero S, Michelis MB, Riganti S. Use of the eight-plate for angular correction of knee deformities due to idiopathic and pathologic physis: initiating treatment according to etiology. J Child Orthop. 2011; 5:209–216. [PubMed: 22654982]
18. Stevens PM. Guided growth: 1933 to the present. Strat Traum Limb Recon. 2006; 1:29–35.
19. Burnette JB, et al. Incidence of inpatient surgeries in children and young adults with childhood orthopedic diagnoses. J Pediatr Orthop. 2004; 24:738–741. [PubMed: 15502580]
20. Sturm PF, Anadio JM, Dede O. Recent advances in the management of early onset scoliosis. Orhop Clin N Am. 2014; 45:501–514.
21. Betz RR, et al. Vertebral body stapling: a fusionless treatment option for a growing child with moderate idiopathic scoliosis. Spine. 2010; 35:169–176. [PubMed: 20081512]
22. Samdani AF, et al. Anterior vertebral body tethering for immature adolescent scoliosis: on year results on the first 32 patients. Eur Spine J. 2015; 24:1533–1539. [PubMed: 25510515]
23. Daerden F, Lefeber D. Pneumatic artificial muscles: actuators for robotics and automation. European Journal of Mechanical and Environmental Engineering. 2002; 47(1)
24. Wang Y, Ameer GA, Sheppard BJ, Langer R. A tough biodegradable elastomer. Nat Biotechnol. 2002; 20(6):602–606. [PubMed: 12042865]
25. Doumit M, Fahim A, Munro M. Analytical modeling and experimental validation of the braided pneumatic muscle. IEEE Trans Robot. 2009; 25(6):1282–1291.
26. Wang Y, Kim YM, Langer R. Technical note: *in vivo* degradation characteristics of poly(glycerol sebacate). J Biomed Mater Res. 2003; 66A:192–197.
27. Pomerantseva I, et al. Degradation behavior of poly(glycerol sebacate). J Biomed Mater Res. 2009; 91A:1038–1047.
28. Stokes IAF, Aronsson DD, Dimock AN, Cortright V, Beck S. Endochondral growth in growth plates of three species at two anatomical locations modulated by mechanical compression and tension. J Orthop Res. 2006; 24:1327–1334. [PubMed: 16705695]
29. Sundback CA, et al. Biocompatibility analysis of poly(glycerol sebacate) as a nerve guide material. Biomaterials. 2005; 26:5454–5464. [PubMed: 15860202]
30. Greenwald D, Shumway S, Albear P, Gottlieb L. Mechanical comparison of 10 suture materials before and after *in vivo* incubation. J Surg Res. 1995; 56(4):372–377.Thorac Cardiovasc Surg Pediatr Card Surg Annu. 2011; 14:75–84.
31. Bylski-Austrow DI, Wall EJ, Rupert MP, Roy DR, Crawford AH. Growth plate forces in the adolescent human knee: a radiographic and mechanical study of epiphyseal staples. J Pediatr Orthop. 2001; 21:817–823. [PubMed: 11675562]
32. Siefert AW, et al. *In-vivo* mitral annuloplasty ring transducer: implications for implantation and annular downsizing. J Biomech. 2013; 46(14):2550–2553. [PubMed: 23948375]
33. Sun Z, et al. Glycolic acid modulates the mechanical property and degradation of poly(glycerol, sebacate, glycolic acid). J Biomed Mat Res Part A. 2010; 92A:332–339.
34. Colan SD. The why and how of Z scores. J Am Soc Echocardiogr. 2013; 25:1–2.

35. Dimeglio A, Canavese F. The growing spine: how spinal deformities influence normal spine and thoracic cage growth. Eur Spine J. 2012; 21:64–70. [PubMed: 21874626]

36. Wolford LM, Movahed R, Perez DE. A classification system for conditions causing condylar hyperplasia. J Oral Maxillofac Surg. 2014; 72:567–595. [PubMed: 24388179]

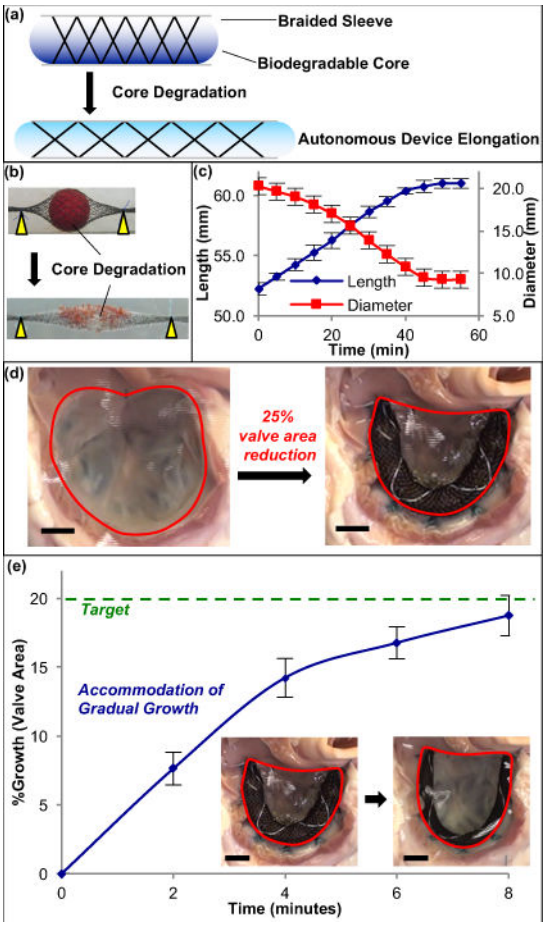

Figure 1. Growth-accommodating device concept – accelerated degradation model of biaxially braided sleeve and biodegradable core

a, Schematic of degradable polymer core (*blue*) placed inside braided sleeve to control sleeve diameter, coupling inner polymer degradation to braided sleeve (and overall device) elongation. **b**, Dissolvable spherical sucrose core (*red*) inside nitinol biaxial braid acts as degradable polymer surrogate. When submerged in water gradual core dissolution leads to gradual decrease in braided sleeve diameter and concomitant autonomous 1-D device elongation for long-bone orthopedic applications. **c**, Braided sleeve behavior & core degradation. Device elongation is gradual and reproducible, and is dependent upon core diameter change (n = 4, mean ± s.d.). **d**, *En face* view of tricuspid valve in isolated swine heart preparation. Annuloplasty using growth-accommodating ring prototype results in 25% reduction in valve area (877.2 ± 141.2 mm^2 → 650.6 ± 55.3 mm^2). **e**, Ring & valve growth. When placed in water, core dissolution enables braided sleeve elongation and gradual ring expansion, allowing for controlled heart valve growth to target valve area of 780 mm^2 (20% growth) (n = 3, mean ± s.d.). Scale bars = 10 mm.

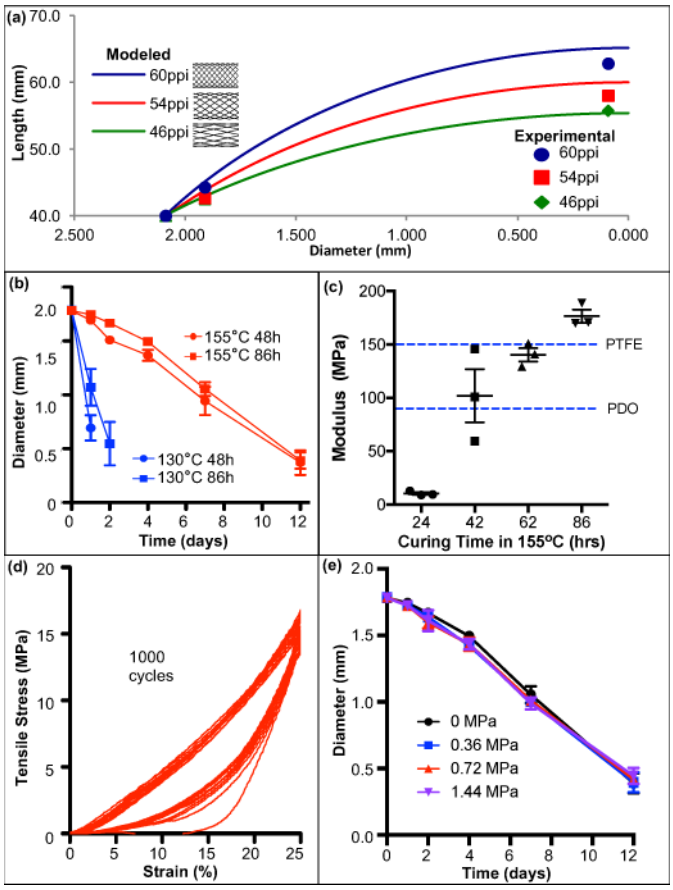

Figure 2. Biaxially braided sleeve, inner polymer, and overall device characterization

a, Braid elongation (modeled vs. experimental). Graphical representation of length-diameter relationship for biaxially braided sleeves. Changing braid pitch (defined by picks-per-inch (PPI)) creates unique elongation profiles for device tunability. Modeled braided sleeve behavior (curves) accurately reflects actual sleeve behavior (experimentally measured lengths: ◆, ■, ●) across range of braid profiles. **b**, ESPGS degradation profile under accelerated conditions for different polymer curing temperatures & durations. Degradation rate is significantly influenced by curing temperature (n = 3, mean ± s.d.). **c**, Young's modulus of device with different PGS cores. Overall device modulus is affected by inner polymer curing. Increasing curing duration and curing at 155°C results in increased device strength. Device prototypes with 86-hour ESPGS have greater Young's Modulus than commercially available surgical sutures (e.g. PTFE, polydioxanone (PDO)) (n = 3, mean ± s.d.). **d**, Representative cyclic tensile testing demonstrates no evidence of device fatigue following 1000 cycles (n = 3). **e**, ESPGS degradation profile under accelerated conditions with varying tensile stresses applied to overall device. Degradation rate is not significantly influenced by applied stress. (n = 3, mean ± s.d.)

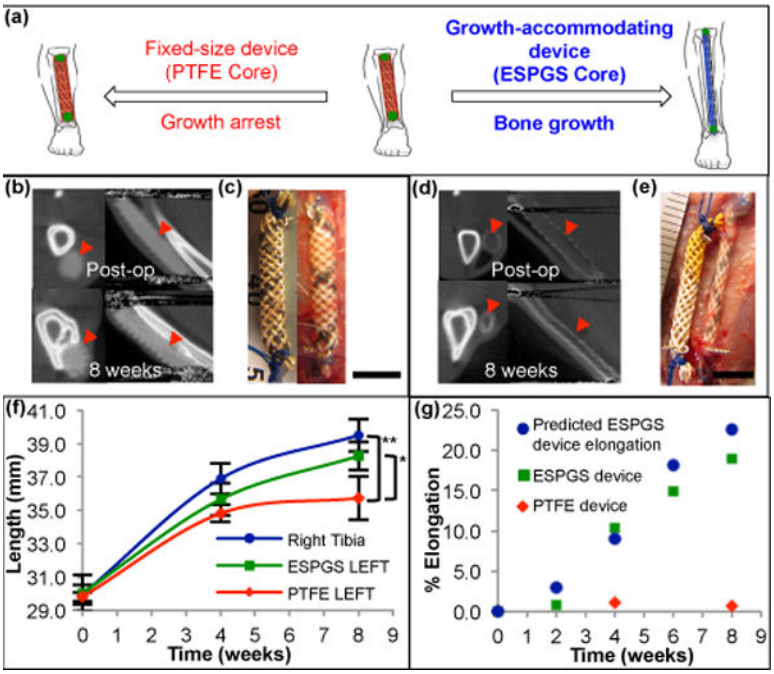

Figure 3. Growing rat musculoskeletal model demonstrating growth restriction with fixed-size implant and growth accommodation with autonomously elongating implant

a, Cartoon depicting device implant on the growing tibia. Use of degradable core enables growth accommodation and guided tibial growth (right). Use of nondegradable core results in fixed-size implant and restricted tibial growth (left). **b**, Micro-CT images in axial (left) & sagittal (right) cross-section show fixed size of PTFE device (◤) and absence of device elongation over 8-week survival. **c**, Comparison of fixed-size device at implant (left) and explant (right) shows no significant change in device length (scale bar = 5 mm). **d**, Micro-CT images of growth-accommodating device show thinning of ESPGS and concurrent lengthening of device (◤) over 8-week survival. **e**, Comparison of growth-accommodating device at implant (left) and explant (right) shows significant device elongation (scale bar = 5 mm). **f**, Tibial growth. Implantation of growth-accommodating device (ESPGS core) versus fixed-size device (PTFE core) led to distinct growth profiles (mean ± s.d.). Fixed-size implant caused progressive growth restriction and ultimately growth arrest in the final 4 weeks (◆). Growth-accommodating implant provided mild growth restriction during first 4 weeks, but permitted physiologic bone growth in last 4 weeks (■). By 8 weeks, left tibial length with fixed-size implant was statistically less than left tibial length with growth-accommodating implant and right tibial length (●) (* P = 0.037, ** P = 0.004, one-way ANOVA post-hoc Tukey test). (n = 3 animals per group) **g**, Comparison of predicted and observed device elongation in representative animals. Observed ESPGS device elongation (■) closely correlated with predicted elongation (●). Fixed-size implant (◆) shown for comparison.

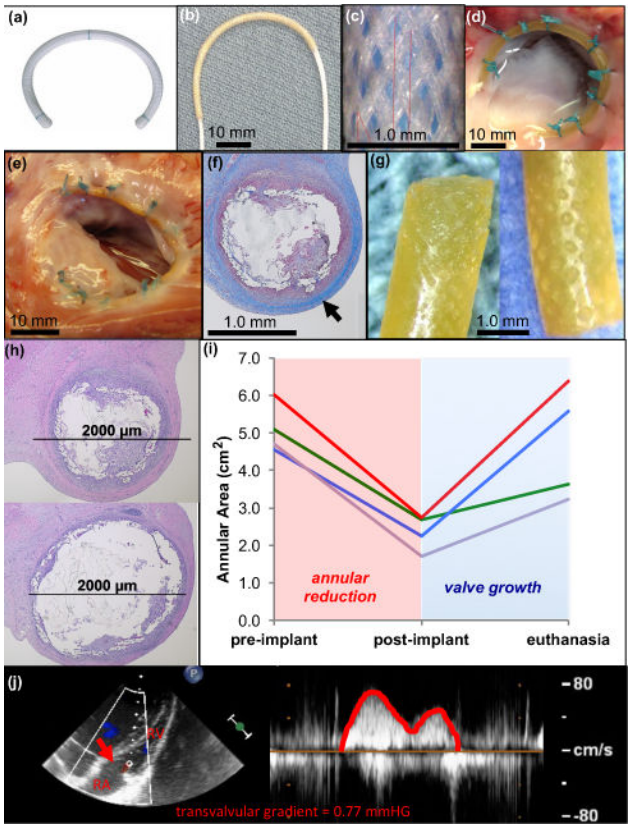

Figure 4. Growing piglet heart valve proof-of-concept - exploring use of growth-accommodating annuloplasty device in a dynamic cardiovascular environment

a, Commercially available fixed-size annuloplasty device used in adults. **b**, UHMWPE biaxially braided sleeve placed over pre-curved cylindrical ESPGS polymer core. **c**, Biaxially braided sleeve pattern. **d**, *Ex vivo* demonstration of ring implantation with *en face* view of tricuspid valve. Growth-accommodating ring is secured to valve annulus with conventional suturing technique used for ring implantation in adults. UHWPE braided sleeve ends and body of device are secured to annulus. **e**, *En face* view of freshly explanted tricuspid valve and ring 12 weeks after surgery. Ring is intact and integrated into annular tissue without evidence of thrombus formation or dehiscence. **f**, Cross-section through explanted ring demonstrating collagen layer that grew over device (↗). **g**, Explanted ESPGS samples demonstrate erosion at polymer surface. **h**, Cross-sections through segments of ring/annulus demonstrate regions of significant core erosion with ring thinning *(top)* and areas of less significant core erosion with less thinning of ring *(bottom)*. **i**, Tricuspid valve area at three study points: pre-implant, post-implant, and euthanasia. All animals experienced valve reduction following ring implantation (red region), and experienced valve growth in the post-operative period (blue region). (GREEN line: 5 week animal, RED line: 12 week animal, BLUE line: 16 week animal, PURPLE line: 20 week animal) **j**, Continuous wave color Doppler echocardiogram demonstrates only trivial gradient (0.77 mmHg) across tricuspid valve orifice (↗) at time of euthanasia, indicating that growth-accommodating ring did not induce valve stenosis after implantation. RA = right atrium, RV = right ventricle.